Numeric and variational study of the anisotropic Heisenberg antiferromagnet interacting with a magnetic field

David Gottlieb, Maximiliano Montenegro, and Miguel Lagos
Departamento de Física, Facultad de Ciencias, Universidad de Chile, Casilla 653, Santiago, Chile

Karen Hallberg
Centro Atómico de Bariloche, Instituto Balseiro, Comisión Nacional de Energía Atómica, 8400 San Carlos de Bariloche, Río Negro, Argentina
(Received 3 December 1991)

We present a variational approach to the Heisenberg antiferromagnetic model for spin $\frac{1}{2}$ and anisotropic exchange, with an external longitudinal and transverse magnetic field. In the one-dimensional case, we calculate exactly with our trial function the expectation values of energy, sublattice magnetization, and magnetic susceptibility. On minimizing the energy, we obtain several phases, which depend on the strength of the field and anisotropy parameter. Subsequently we approach the problem numerically and solve it for a chain of 12 spins using the Lanczos method. The two approaches are in excellent concordance, particularly for the critical fields of the transitions, over a wide range of the parameters of the model. Beside its precision and mathematical simplicity, the method has the important advantage of accounting for the different magnetic phases and their transitions with a single trial function that has a compact mathematical expression. The formalism is expected to work better in higher dimensions, but the corresponding calculations are omitted because of the lack of numerical field-dependent data with which to compare.

I. INTRODUCTION

The discovery of magnetic order in the superconducting layered perovskites[1-3] has motivated a surge of interest in the study of quantum Heisenberg models. In the recent literature on the subject[4], there are many advances over the models that were originally formulated, as well as extensions of them intended to interpret the physics of the superconducting ceramics. This effort has produced several recent approximate formulations[5-14] aimed to gain insight into the ground-state properties of the antiferromagnetic model, which are far from straightforward even when the exact solution is known from Bethe's ansatz. The exact solutions for the ground state in one dimension, known analytically if there is no external field,[15-17] and numerically for large clusters with a finite field,[18] constitute major achievements but have the disadvantage of dealing with major and minor terms on the same footing. This obscures their physical implications and often makes them impractical for further calculations. These shortcomings, and the necessity of a general scheme able to be extended to more than one dimension, confer interest on approximate approaches. Most of the work has been on two-dimensional models since the discovery of long-ranged antiferromagnetic correlations in the CuO_2 planes of the superconducting cuprates.[3]

It has been proved recently that the physics of the antiferromagnetic Heisenberg model with no external field can be described neatly by a class of nonmagnetic excitations, constructed with paired spin operators.[5,19-28] The corresponding approximate theory, which we will call hereafter *paired nonmagnetic excitations* (PNME) theory, clearly differs from conventional spin-wave theory because it introduces singlet magnetic excitations, as opposed to the triplet antiferromagnetic magnons of the latter. The idea of using magnon-paired states was introduced by Manousakis[9] at the same time the basic concepts of the PNME theory appeared in the literature. The two approaches were developed independently and differ in formal aspects. However, the essential physical idea underlying both seems to be the same, which was made explicit by Manousakis.[9]

The PNME theory assumes antiferromagnetic order and proves to be notably accurate when this hypothesis is actually realized by the system. Hence the applicability of the method in one dimension is restricted to anisotropic coupling with anisotropy toward the Ising limit ($\alpha < 0.5$) and loses precision when approaching the isotropic limit ($\alpha = 1$).[20] In two dimensions, the antiferromagnetic order prevails for anisotropies that range from the Ising to the isotropic Heisenberg models ($0 \leq \alpha \leq 1$), and the approximate approach works exceedingly well, much better than linear spin-wave theory, for all values of α in this range.[23]

In addition to its accuracy and mathematical simplicity, the PNME theory has shown to be flexible enough to be easily generalized to arbitrary dimension,[23] spin,[5] and nonfrustrating second-next-nearest-neighbor interactions.[24,26] The extension to exchange anistropy toward the XY limit ($\alpha > 1$) has been made.[28] Specifically, for two dimensions, isotropic exchange and $S = \frac{1}{2}$, the ground-state energy deviates less than 0.5% from the results given by elaborate Monte Carlo calculations.[29] On reducing the anisotropy parameter α, the error becomes even smaller.

In this work we address the Heisenberg antiferromagnetic model for spin $\frac{1}{2}$ and anisotropic exchange in external longitudinal and transverse magnetic fields. First, we employ a variational approach that uses as trial function a version of the analytic expression for the ground state given by the PNME theory, generalized in order to incorporate the external field. The calculations are done in one dimension but can be extended to arbitrary dimension by the method described in Ref. 23. The ground-state energy, sublattice magnetization, and magnetic susceptibility are obtained. Subsequently we approach the problem numerically and solve it for a chain of 12 spins using the Lanczos method.[30,31]

The two approaches have excellent concordance over a wide range of the parameters of the model. We show that our analytic trial function represents accurately the ground state of the system for anisotropies ranging from the Ising limit to the almost-isotropic Heisenberg model for all values of the field. Moreover, it accounts for the several antiferromagnetic and ferromagnetic phases occurring for different values of the magnetic field with the same precision. The critical fields of the transitions are also predicted correctly. All the calculations of the variational theory in one dimension are exact and analytical.

It has been shown in a previous paper that the expression for the ground state used here in one dimension is generalizable to higher dimensionalities with a large gain in accuracy.[5,23,28] Hence we conclude that our variational ground state also represents well the physics of the model in more than one dimension. We omit here these calculations because of the lack of reliable field-dependent numerical data in two or more dimensions with which to compare them. We must mention, however, that the success of our trial function in one dimension makes its extension to more than one dimension highly reliable.

II. THE MODEL AND PNME TREATMENT OF IT

Assuming a bipartite lattice the Hamiltonian of the $S=\frac{1}{2}$ Heisenberg antiferromagnet, with anisotropic exchange interaction and immersed in a magnetic field $\mathbf{H}$, can be written as

$$\mathcal{H}=J\sum_{\mathbf{r},\delta}\left[S_z(\mathbf{r})S_z(\mathbf{r}+\delta)+\frac{\alpha}{2}[S_+(\mathbf{r})S_-(\mathbf{r}+\delta)+S_+(\mathbf{r}+\delta)S_-(\mathbf{r})]\right] -g\mu_B\sum_{\mathbf{r}}[H_xS_x(\mathbf{r})+H_zS_z(\mathbf{r})+H_xS_x(\mathbf{r}+\delta)+H_zS_z(\mathbf{r}+\delta)] , \tag{1}$$

where S_x, S_y, S_z denote the components of the spin associated to the lattice site settled in their arguments, $S_\pm=S_x\pm iS_y$, and α is a parameter determining the anisotropy of the interaction between the spins. The magnetic field is constrained to lie in the xz plane. Vectors $\mathbf{r}$ characterize the sites of one of the two sublattices defined by the antiferromagnetic order and δ connects a site with any of its z nearest neighbors. This way $\mathbf{r}$ and $\mathbf{r}+\delta$ are in different sublattices, for any $\mathbf{r}$ and δ.

To make clear the physical foundation of our trial function we review here briefly the main results of the PNME theory[5,19–28] for the antiferromagnetic Heisenberg model with zero magnetic field, whose ground state is used as the starting point in the subsequent variational approach. We define the zN 0-spin operators[5]

$$\phi_\delta^\dagger(\mathbf{k})=\frac{1}{\sqrt{2S^2N}}\sum_{\mathbf{r}}e^{i\mathbf{k}\cdot\mathbf{r}}S_+(\mathbf{r}+\delta)S_-(\mathbf{r})+Q\delta_{\mathbf{k},0} , \tag{2}$$

where

$$Q=\left[\frac{N}{2}\right]^{1/2}\frac{\alpha S}{(2zS-1)} . \tag{3}$$

In Eq. (2) the wave vector $\mathbf{k}$ is in the Brillouin zone of one of the two sublattices. The expressions for the commutation relations satisfied by the ϕ operators are in general quite involved. However, it can be shown that in the asymptotic regime of high antiferromagnetic order ($\alpha<1$), they reduce to[5,23]

$$[\phi_\delta(\mathbf{k}),\phi_{\delta'}(\mathbf{k}')]=0 ,$$
$$[\phi_\delta(\mathbf{k}),\phi_{\delta'}^\dagger(\mathbf{k}')]=\delta_{\mathbf{k},\mathbf{k}'}\delta_{\delta,\delta'} , \tag{4}$$

$$[\mathcal{H},\phi_\delta^\dagger(\mathbf{k})]=(2zS-1)J\phi_\delta^\dagger(\mathbf{k}) . \tag{5}$$

Therefore, in this approximation the ϕ operators represent Bose excitations of the Heisenberg model. The PNME theory follows from using the above simple commutation relations instead of the true ones. The ultimate justification of this deceptively crude procedure is its success which has proved to be remarkable. The Hamiltonian then turns into[5,23]

$$\mathcal{H}=(2zS-1)J\sum_{k,\delta}\phi_\delta^\dagger(\mathbf{k})\phi_\delta(\mathbf{k})+E_g , \tag{6}$$

where

$$E_g=-\frac{N}{2}JzS^2-\frac{NJzS^2\alpha^2}{2(2zS-1)} \tag{7}$$

is the ground-state energy. It should be noticed, however, that the ϕ operators only revert pairs of antialigned spins and cannot change the total spin. Thus one cannot construct states with finite spin with them. This way the description of the spin dynamics provided by the PNME theory is restricted only to the manifold of states with zero total spin. For the same reason, it is not adequate to account for the dynamical consequences of the interaction with an external magnetic field. In this sense the Hamiltonian (6) is incomplete because it drops the spin-carrying excitations, which are necessary to span the full Hilbert space of states.

The ground state $|g(\alpha)\rangle$ is determined by the set of equations

$$\phi_\delta(\mathbf{k})|g(\alpha)\rangle=0 , \tag{8}$$

for any $\mathbf{k}$ and δ. Using the approximate commutation relations of the ϕ operators, it is not difficult to show that the state[5,23]

$$|g(\alpha)\rangle=\exp\left[-Q\sum_\delta[\phi_\delta^\dagger(0)-\phi_\delta(0)]\right]|\mathcal{N}\rangle \tag{9}$$

satisfies them and is thus the ground state of the approximate theory. The excited states with zero total spin are then

$$|\{n_{\delta k}\}\rangle=\prod_{\delta,k}\frac{[\phi_\delta(\mathbf{k})]^{n_{\delta k}}}{\sqrt{n_{\delta k}!}}|g(\alpha)\rangle,\quad n_{\delta k}=0,1,\ldots\ . \tag{10}$$

The utility of having the stationary states greatly depends on the knowledge of how to calculate matrix elements with them. For $S=\frac{1}{2}$ and one dimension we developed a method that allows us to calculate exact closed-form expressions for the mean value of any operator with respect to the ground state (9). The procedure is described in Ref. 20 and can be used to derive the formulas

$$\langle g(\alpha)|S_z(l)S_z(l+1)|g(\alpha)\rangle=-\tfrac{1}{4}[J_0^2(2\alpha)+J_1^2(2\alpha)]\ , \tag{11}$$

$$\langle g(\alpha)|[S_+(l)S_-(l+1)+S_+(l+1)S_-(l)]|g(\alpha)\rangle=-J_1(2\alpha)\ , \tag{12}$$

and

$$\langle g(\alpha)|S_z(l)|g(\alpha)=[(-1)^l/2]J_0(2\alpha)\ , \tag{13}$$

where $J_n(x)$ is the Bessel function of order n, which will be of use in what follows. For higher spin or dimensionality, one can resort to finite expansions in powers of α.

Before we extend the former results for nonvanishing magnetic field it is convenient to call attention to a simple but important property of the ground and excited states (9) and (10) of the PNME theory. All these states can be expressed as sums of terms of the form

$$[\phi_\delta^\dagger(\mathbf{k})]^n[\phi_{\delta'}(\mathbf{k}')]^m|\mathcal{N}\rangle\ . \tag{14}$$

On the other hand, the ϕ operators can only revert pairs of antialigned spins and, denoting

$$S_z^T=\sum_{\mathbf{r}}[S_z(\mathbf{r}+\boldsymbol{\delta})+S_z(\mathbf{r})] \tag{15}$$

the total spin, one finds

$$S_z^T[\phi(\mathbf{k})_\delta^\dagger]^n[\phi(\mathbf{k}')_{\delta'}]^m|\mathcal{N}\rangle=0\ , \tag{16}$$

for any n and m. The same applies to the states (9) and (10), and

$$S_z^T|g(\alpha)\rangle=S_z^T|\{n_{\delta k}\}\rangle=0\ . \tag{17}$$

Hence the ground and excited states not only give $\langle S_z^T\rangle=0$ but, furthermore, are entirely contained in the subspace of states $\mathcal{S}(0)$ spanned by the eigenvectors of S_z^T with eigenvalue zero. Consequently, our approximate eigenstates of $\mathcal{H}$ are orthogonal to any vector in the orthogonal subspaces $\mathcal{S}\pm(\frac{1}{2}),S(\pm1),\ldots$. This way we have, in particular, that

$$\langle g(\alpha)|S_+(\mathbf{r}+\boldsymbol{\delta})S_+(\mathbf{r}')|g(\alpha)\rangle=\langle g(\alpha)|S_-(\mathbf{r}+\boldsymbol{\delta})S_-(\mathbf{r}')|g(\alpha)\rangle=0\ , \tag{18}$$

and

$$\langle g(\alpha)|S_z(\mathbf{r}+\boldsymbol{\delta})S_\pm(\mathbf{r}')|g(\alpha)\rangle=0\ . \tag{19}$$

III. TRIAL STATES FOR FINITE EXTERNAL FIELD AND ENERGY FUNCTIONAL

Turn now to the generalization to $\mathbf{H}\neq0$, which is our main present purpose. It can be observed in the correlation functions (11), (12), and (13) that the ground state represents essentially a chain of spins oriented antiferromagnetically in the z direction with sublattice magnetization diminished by quantum fluctuations. When applying a small magnetic field, say, in the x direction, it is expected that the direction of the spins will change by a small amount. Consider then the trial state

$$|g(\theta_1,\theta_2,\alpha')\rangle=R_y(\theta_1,\theta_2)|g(\alpha')\rangle\ , \tag{20}$$

where the unitary operator

$$R_y(\theta_1,\theta_2)=\prod_{\mathbf{r}}\exp[i\theta_1S_y(\mathbf{r}+\boldsymbol{\delta})]\exp[i\theta_2S_y(\mathbf{r})] \tag{21}$$

represents a rotation of the spins in the two sublattices by angles θ_1 and θ_2, respectively, around the y axis. Vector $\boldsymbol{\delta}$ is any of the z vectors connecting adjacent sites. In this scheme θ_1, θ_2, and α' are variational parameters and the energy functional is

$$F(\theta_1,\theta_2,a')=\langle g(\alpha')|R_y^\dagger(\theta_1,\theta_2)\mathcal{H}R_y(\theta_1,\theta_2)|g(\alpha')\rangle\ . \tag{22}$$

Taking advantage of the unitary character of the operators $R_y(\theta_1,\theta_2)$, one can reinterpret Eq. (22) as the expectation value of the transformed operator $R_y^\dagger\mathcal{H}R_y$ with respect to the states $|g(\alpha')\rangle$, with which we already know how to work. To accomplish the transformation, just substitute in Eq. (1)

$$\begin{aligned}S_x&\rightarrow\cos\theta S_x-\sin\theta S_z\ ,\\ S_y&\rightarrow S_y\ ,\\ S_z&\rightarrow\sin\theta S_x+\cos\theta S_z\ ,\end{aligned} \tag{23}$$

with $\theta=\theta_1$ and $\theta=\theta_2$ for sites in the spin-up and spin-down sublattices, respectively. Then substitute the resulting expression in place of $R_y^\dagger\mathcal{H}R_y$ in Eq. (22). Recalling that $S_x=(S_++S_-)/2$ and $S_y=(S_+-S_-)/(2i)$ and Eqs. (18) and (19), one readily arrives at

$$\frac{F(\theta_1,\theta_2,\alpha')}{NJ}=(\cos\theta_1\cos\theta_2+\alpha\sin\theta_1\sin\theta_2)H_I(\alpha')+\tfrac{1}{4}(\alpha+\alpha\cos\theta_1\cos\theta_2+\sin\theta_1\sin\theta_2)H_{xy}(\alpha')$$
$$+\tfrac{1}{2}[(\sin\theta_1-\sin\theta_2)h_x+(\cos\theta_1-\cos\theta_2)h_z]M_z(\alpha')\ , \tag{24}$$

where $h_z \equiv g\hbar\mu_b H_z/J$, and $h_x \equiv g\hbar\mu_b H_x/J$ are the components of the reduced magnetic field. The coefficients

$$H_I(\alpha') = \langle g(\alpha') | S_z(l) S_z(l+1) | g(\alpha') \rangle \ , \tag{25}$$

$$H_{xy}(\alpha') = \langle g(\alpha') | [S_+(l) S_-(l+1) + S_+(l+1) S_-(l)] | g(\alpha') \rangle \ , \tag{26}$$

and

$$M_z(\alpha') = \langle g(\alpha') | S_z(l) | g(\alpha') \rangle \tag{27}$$

do not depend on θ_1 and θ_2, but only on α'. In one dimension they can be put in explicit form by using Eqs. (11)–(13).

Our problem then reduces to minimizing with respect to θ_1, θ_2, and α'. We study the two interesting cases of transversal and parallel magnetic field separately.

IV. SOLUTION FOR TRANSVERSE MAGNETIC FIELD

For external magnetic field oriented along the x axis, perpendicular to the preferred direction of the spins, the extremum equations for θ_1, θ_2, and α' become

$$\sin\xi \left[(1-\alpha) \left[\frac{1}{4} H_{xy} - H_I \right] \cos\xi - \frac{M_z h_x}{2} \sin\eta \right] = 0 \ , \tag{28}$$

$$\cos\eta \left[(1+\alpha) \left[\frac{1}{4} H_{xy} + H_I \right] \sin\eta - \frac{M_z h_x}{2} \cos\xi \right] = 0 \ , \tag{29}$$

and

$$\frac{\alpha}{2\alpha'} H_{xy}^2 - \frac{1+\alpha}{4\alpha'} H_{xy} - (1+\alpha) M_z - (1+\alpha) \left[\frac{H_{xy}^2}{2\alpha'} - \frac{H_{xy}}{4\alpha'} - M_z \right] \sin^2\eta + (1-\alpha) \left[\frac{H_{xy}^2}{2\alpha'} + \frac{H_{xy}}{4\alpha'} + M_z \right] \cos^2\xi + H_{xy} h_x \sin\eta \cos\xi = 0 \ , \tag{30}$$

where we have defined the new variables η and ξ as

$$\xi = \tfrac{1}{2}(\theta_1 + \theta_2), \quad \eta = \tfrac{1}{2}(\theta_1 - \theta_2) \ . \tag{31}$$

The α' dependence is entirely contained in the factors $H_I(\alpha')$, $H_{xy} = H_{xy}(\alpha')$, and $M_z = M_z(\alpha')$.

This set of equations has four solutions. One of them, giving the absolute minimum of F, is the only physical one. However, the set of physical values for the variational parameters may correspond, in principle, to any of the four solutions as the strength of the field is varied. Crossovers yielding phase transitions are thus conceivable. We have the following:

(a) the first solution of Eqs. (28)–(30),

$$\xi = 0, \quad \sin\eta = \frac{2 M_z h_x}{(1+\alpha)(H_{xy} + 4H_I)} \ , \tag{32}$$

in the limit $h_x \ll 1$ represents an antiferromagnetic state slightly deviated from the z axis in the direction of the magnetic field. It is expected to produce an absolute minimum of the energy for small h_x and α. In this situation, $\alpha' \approx \alpha$ and the rotation angles become

$$\theta_1 \approx \frac{2 M_z h_x}{(1+\alpha)(H_{xy} + 4H_I)} \ , \qquad \theta_2 \approx \frac{-2 M_z h_x}{(1+\alpha)(H_{xy} + 4H_I)} \ . \tag{33}$$

(b) The second solution is

$$\xi = 0, \quad \eta = \pi/2 \ . \tag{34}$$

It corresponds to a ferromagnetic configuration (θ_1 and θ_2 are measured from the antiferromagnetic state) and is expected to give the absolute minimum of the energy functional for high values of the magnetic field. In this limit $\alpha' \to 0$.

(c) The solution

$$\xi = \pi/2, \quad \eta = 0 \tag{35}$$

represents an antiferromagnetic configuration in the $x-y$ plane. It is expected to yield the absolute minimum of energy for small magnetic fields and $\alpha > 1$.

(d) The last solution,

$$\xi \neq 0, \quad \eta = \pi/2 \ , \tag{36}$$

never gives an absolute minimum of the mean energy.

We solved Eqs. (28)–(30) numerically for a number of values of the reduced magnetic field h_x. The energy was then evaluated for each of the four solutions. Figure 1 shows the results for exchange anisotropy $\alpha = 0.5$, depicted as functions of the strength of the reduced magnetic field. The mean energies given by the different solutions are labeled (a), (b), (c), and (d). The curve associated to the absolute minimum of the energy functional, representing the true energy, is composed of two parts determined by the crossover at $h_x \approx 1.3$ of the solutions (a) and (b). It is seen that at this point the solution changes smoothly from an antiferromagnetic configuration to a ferromagnetic one as the magnetic field increases. In the high-field regime α' decreases to zero, while θ_1 and θ_2 go to $\pi/2$ and $-\pi/2$, respectively.

Figure 2 displays the same as Fig. 1 but for $\alpha = 1.5$. This corresponds to anisotropy toward the XY sector of the anisotropic Heisenberg model. The results of Fig. 2

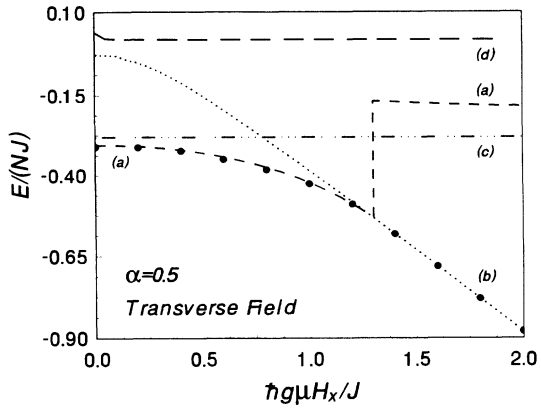

FIG. 1. Ground-state energy of the Heisenberg antiferromagnet in one dimension as a function of the external magnetic field H_x, whose direction is perpendicular to the z direction, characterized by the anisotropy of the exchange interaction between the spins. Dimensionless magnitudes are used. The anisotropy parameter $\alpha=0.5$ corresponds to a situation intermediate between the Ising ($\alpha=0$) and isotropic ($\alpha=1$) Heisenberg models. Two of the four sets of field-dependent variational parameters, denoted (a), (b), (c), and (d), extreming the energy functional participate in the curve giving the physical energy. They determine two different field-dependent phases of the model at $T=0$. Their precise nature is discussed in Sec. VI. The black circles represent the results of a numerical simulation for a chain of 12 spins.

show an additional transition because a contribution of solution (c) now enters for field strengths below $h_x \approx 1$. The crossover between (a) and (b) is shifted to higher fields.

Figures 1–3 show how the ground-state energy of the variational calculation compares with computer-generated data, represented by the discrete points, for several choices of the anisotropy parameter α. The computational approach is based in the Lanczos method and

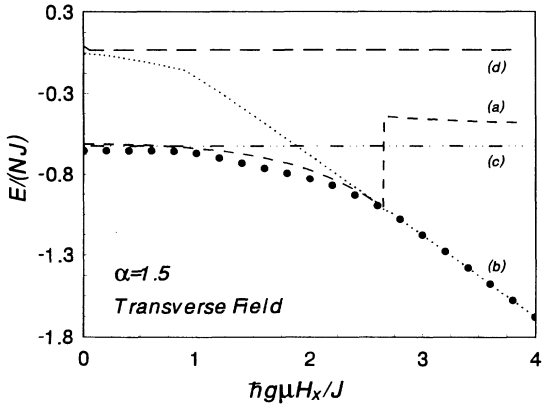

FIG. 2. Same as Fig. 1, but for $\alpha=1.5$, which corresponds to anisotropy toward the XY limiting model ($\alpha \to \infty$). Three of the four solutions of the extremum equations contribute now to the physical energy for different values of the external field H_x. The system exhibits three phases at $T=0$.

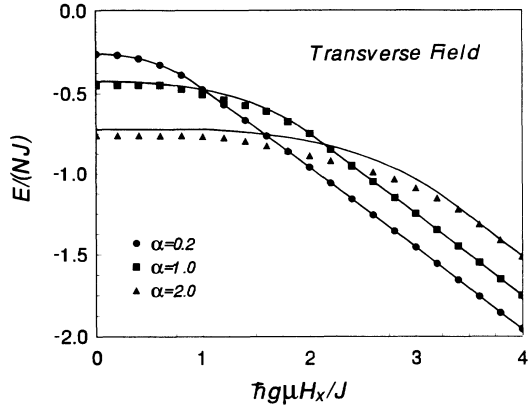

FIG. 3. Ground-state energy as a function of the strength of the external transverse field, for isotropic exchange interaction ($\alpha=1$) and two anisotropic situations. The magnitudes of the plot are dimensionless. The filled circles, squares, and triangles are the results of numerical simulations and the continuous lines represent the results of the variational theory.

assumes a chain of 12 spins. Details of the numerical procedure are provided in Refs. 30 and 31. Figure 3 omits the different curves associated with the several solutions of the extremum equations and exhibits just the arcs of them corresponding to absolute minima. The agreement between the variational and numeric results is excellent, particularly for small values of α.

The sublattice magnetization, correlation functions, and magnetic susceptibilities are obtained from Eqs. (11), (12), and (13). One has

$$\langle S_z(l)S_z(l+1)\rangle = -\tfrac{1}{8}(H_{xy}^2+4M_z^2-H_{xy})\cos(2\xi) - \tfrac{1}{8}(H_{xy}^2+4M_z^2+H_{xy})\cos(2\eta)\ , \quad (37)$$

$$\langle S_x\rangle = -M_2 \sin\eta \cos\xi\ , \quad (38)$$

and

$$\chi = M_z \frac{\partial}{\partial h_x}(\sin\eta\cos\xi)\ . \quad (39)$$

The former results for $\mathbf{H}=0$ reduce to those obtained in Ref. 20.

V. SOLUTION FOR PARALLEL MAGNETIC FIELD

In this situation $h_x=0$, and the corresponding set of extremal equations

$$\cos\xi\left[(1-\alpha)\left[\frac{1}{4}H_{xy}-H_I\right]\sin\xi-\frac{M_z h_z}{2}\sin\eta\right]=0\ , \quad (40)$$

$$\cos\eta\left[(1+\alpha)\left[\frac{1}{4}H_{xy}+H_I\right]\sin\eta+\frac{M_z h_z}{2}\sin\xi\right]=0\ , \quad (41)$$

and

$$\frac{1}{2\alpha'}H_{xy}^2-\frac{\alpha}{2\alpha'}H_{xy}-2\alpha M_z-(1+\alpha)\left[\frac{H_{xy}^2}{2\alpha'}-\frac{H_{xy}}{4\alpha'}-M_z\right]\sin^2\eta$$
$$-(1-\alpha)\left[\frac{H_{xy}^2}{2\alpha'}+\frac{H_{xy}}{4\alpha'}+M_z\right]\sin^2\xi-H_{xy}h_z\sin\eta\sin\xi=0\ , \quad (42)$$

has again four solutions:

(a) In the first one,

$$\xi=\eta=0\ , \quad (43)$$

the spins remain oriented antiferromagnetically along the z axis and corresponds to a local minimum of the mean energy. The equation for α',

$$\frac{1}{\alpha'}H_{xy}^2-\frac{\alpha}{2\alpha'}H_{xy}-2\alpha M_z=0\ , \quad (44)$$

has the solution $\alpha'=\alpha$ for small α, which is the relevant case. The ground-state energy, magnetization, and correlation functions correspond to those of the case in which there is no external field and the magnetic susceptibility vanishes.

(b) The second solution,

$$\eta=\frac{\pi}{2},\quad \sin\xi=\frac{2M_zh_z}{(1-\alpha)(H_{xy}-4H_I)}\ , \quad (45)$$

represents a configuration in which the spins of the two sublattices point along the same direction and represent a maximum of energy. The rotation angles are

$$\theta_1\approx\frac{\pi}{2}+\frac{2M_zh_z}{(1-\alpha)(H_{xy}-4H_I)}\ ,$$
$$\theta_2\approx-\frac{\pi}{2}+\frac{2M_zh_z}{(1-\alpha)(H_{xy}-4H_I)}\ , \quad (46)$$

for a weak magnetic field. The spins are ferromagnetically correlated along the x direction and it never gives the absolute minimum of energy.

(c) The third solution,

$$\xi=\frac{\pi}{2},\quad \sin\eta=\frac{-2M_zh_z}{(1-\alpha)(H_{xy}+4H_I)}\ , \quad (47)$$

gives an antiferromagnetic configuration oriented along the x axis. The angles of rotation are

$$\theta_1\approx\frac{\pi}{2}-\frac{2M_zh_z}{(1+\alpha)(H_{xy}+4H_I)}\ ,$$
$$\theta_2\approx\frac{\pi}{2}+\frac{2M_zh_z}{(1+\alpha)(H_{xy}+4H_I)}\ . \quad (48)$$

This solution may correspond to the absolute minimum for $\alpha>1$.

(d) Finally, for

$$\eta=\xi=\pi/2\ , \quad (49)$$

one has that $\theta_1=\pi$ and $\theta_2=0$. Hence the spins align ferromagnetically along the z direction and the solution represents an energy maximum.

Figure 4 shows the expectation value of $\mathcal{H}$ given by the four solutions for $\alpha=0.5$, that is, anisotropy toward the Ising limit. The ground state exhibits three phases, corresponding to solutions (a), (c), and (d), whose physical realization occurs sequentially on increasing the strength of the external field. Figure 5 shows the same situation for $\alpha=1.5$, which corresponds to anisotropy toward the XY model. Just two phases, associated with the solutions (c) and (d), do occur. Figure 6 displays the ground-state energy of the model as a function of the field intensity at

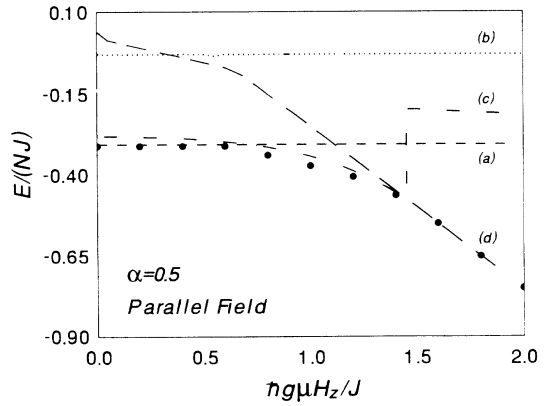

FIG. 4. Ground-state energy in one dimension as a function of an external magnetic field H_z applied in the z direction. The parameter $\alpha=0.5$ corresponds to anisotropy toward the Ising sector. The model exhibits three phases, governed by the solutions (a), (c), and (d), for different strengths of the field. The black circles are numerical results for a chain of 12 spins.

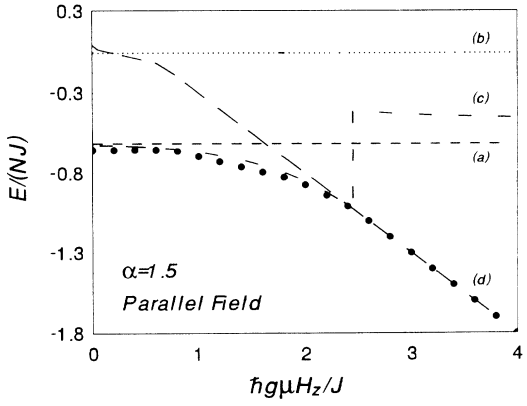

FIG. 5. Same as Fig. 4, but for anisotropy in the XY sector. Just two phases do occur at $T=0$.

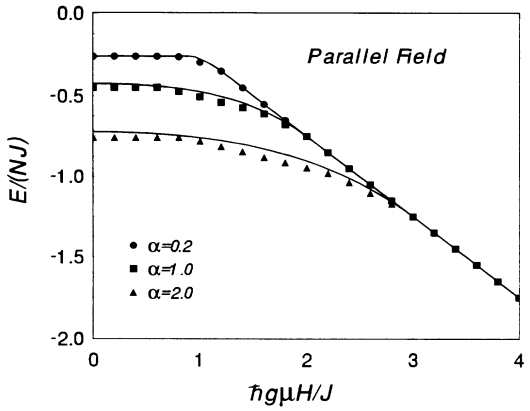

FIG. 6. Same as Fig. 3 but for external field parallel to the direction in which the exchange interaction between the spins is anistropic.

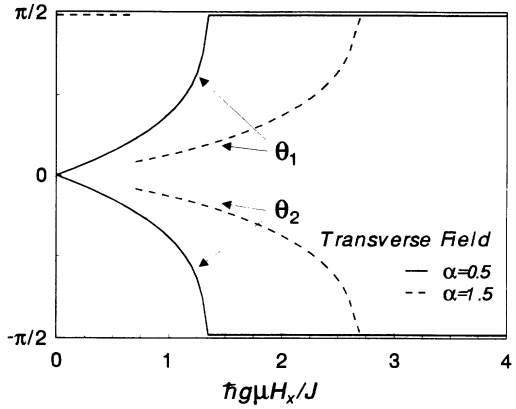

FIG. 7. Mean orientation of the spins in the two sublattices for transverse magnetic field H_x. The angles θ_1 and θ_2, which in our variational scheme are variational parameters, are such that $\theta_1=\theta_2=0$ correspond to an antiferromagnetic configuration oriented along the z axis. For anisotropy toward the Ising sector ($\alpha=0.5$) the spins are antiferromagnetically correlated for $H_x=0$, develop a ferromagnetic component following the field direction as the strength of the latter increases, and then undergo a sudden transition to a true ferromagnetic configuration. For anisotropy toward the XY sector ($\alpha=1.5$) the model at $H_x=0$ is antiferromagnetic in the xy plane. This kind of spin ordering prevails up to a finite value of the field intensity, at which the system jumps to a configuration behaving as in the previous case.

isotropy ($\alpha=1$) and for two anisotropic situations. It is evident that precision increases when approaching the Ising limit.

VI. NATURE OF THE DIFFERENT PHASES IN ONE DIMENSION

The character of the several phases that the model goes through at $T=0$ when varying the strength of the external field can be visualized from the values assumed by θ_1 and θ_2. These are the mean angles subtended by the spins in the two sublattices with respect to a perfect antiferromagnetic configuration oriented along the z axis. This way, for example, $\theta_1=\theta_2$ and $\theta_1=-\theta_2=\pi/2$ correspond to an antiferromagnetic and a ferromagnetic situation, respectively.

Figure 7 shows θ_1 and θ_2 as functions of the intensity of the transverse field for the same anisotropies of Figs. 1 and 2. The exchange anisotropy α determines interesting differences in the behavior of the field-dependent spin ordering. For the enhanced Ising term ($\alpha=0.5$) the system shows a low-field regime in which the spins maintain approximately their antiferromagnetic alignment, but a uniform magnetization arises in the direction of the field as the latter increases. The transition from solutions (a) to (b) of Sec. IV correspond to a transition to a ferromagnetic configuration. The transition is continuous but not smooth. It should be noted that θ_1 and θ_2 establish only the mean orientation of the spins because the ground state (20) incorporates quantum fluctuations, which are in general considerable for $\alpha\neq 0$.

For an enhanced XY term ($\alpha=1.5$) the system has an additional transition. For $h_x=0$ it starts from an antiferromagnetic configuration in the $x-y$ plane and stays in it up to a finite value of the field strength. Then it goes through a discontinuous transition to a new phase. Here the spin components along the z direction exhibit antiferromagnetic order while their x projections have all the same sign. A new transition, now to a true ferromagnetic regime, takes place at a higher field.

Figure 8 plots θ_1 and θ_2 as functions of the strength of a field parallel to the z direction, associated with the anisotropy of the spin-spin interaction. Again the behavior for anisotropies toward the Ising ($\alpha=0.5$) and XY ($\alpha=1.5$) limits exhibits interesting differences. For $\alpha=0.5$ the system has three phases and two transitions. For low parallel fields the spins persist in an antiferromagnetic configuration oriented along the z axis. When the reduced magnetic field increases up to about $h_z=0.7$, the spins jump abruptly to a new configuration, which may be thought of as an antiferromagnetic alignment of

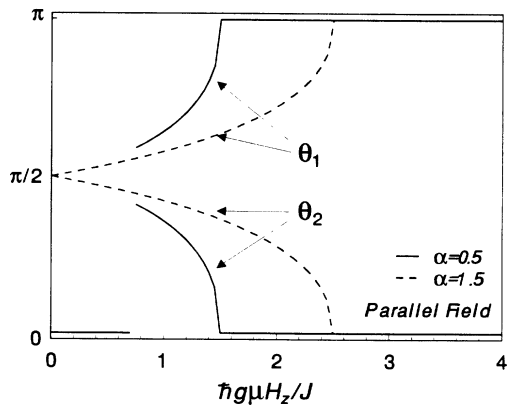

FIG. 8. Same as Fig. 7, but for the direction of the field, which now is parallel to the z axis. Except for a rotation in $\pi/2$, the behavior of the mean orientation of the spins in the two sublattices resembles that of the previous case, in which the field is perpendicular to the x axis.

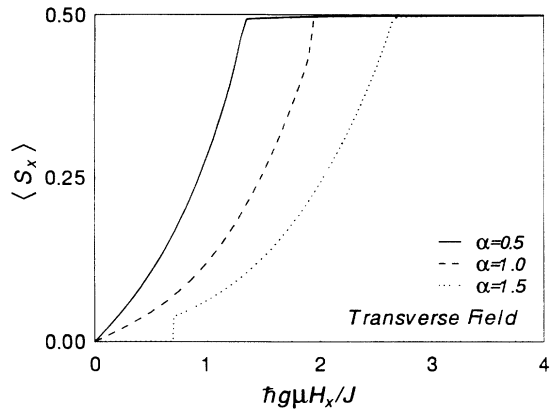

FIG. 9. Magnetization per site in units of $\hbar\mu$ for field external field in the x direction, i.e., perpendicular to the direction in which the exchange interaction between the spins is anisotropic. Notice the discontinuity of the curve for $\alpha=1.5$.

the spin components in the x-y plane together with ferromagnetic order of the z components. The magnetization along the z axis increases with h_z and the system stays in this regime until the reduced parallel field reaches the point $h_z=1.5$, where the x-y antiferromagnetic component disappears and the system goes through a true ferromagnetic phase oriented in the z direction. While the first transition is abrupt, the second is continuous.

For $\alpha=1.5$, that is, anisotropy toward the XY limit, the system behaves quite differently. In agreement with previous results, at $h_z=0$ the system has antiferromagnetic order in the x-y plane. As h_z increases the field causes a ferromagnetic magnetization along the z axis. Close to $h_z=2.5$ the system enters a new phase, in which the spin fluctuate around a perfect ferromagnetic configuration.

Figures 9 and 10 display the magnetization along the field direction for transverse and parallel external fields, respectively.

Figure 11 shows the field-dependent magnetization for a transverse external field, as given by our variational approach (continuous lines) and by the computer simulation (black circles), for three values of the anisotropy parameter α. The computer calculation assumes a chain of 12 sites, which explains the stepped shape of the numerical results. But for this technical aspect both approaches exhibit very good agreement.

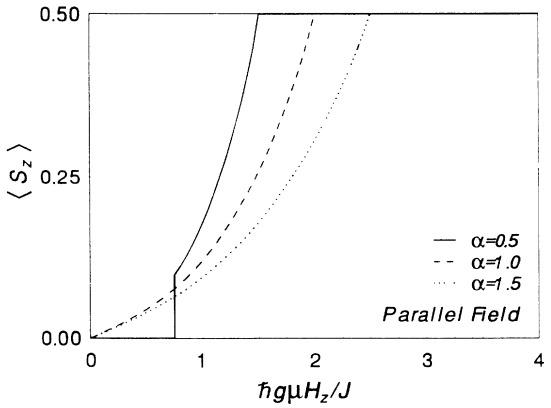

FIG. 10. Same as in Fig. 9, but for the orientation of the field, which in this case is parallel to the z axis. Now the magnetization for $\alpha=0.5$ is discontinuous.

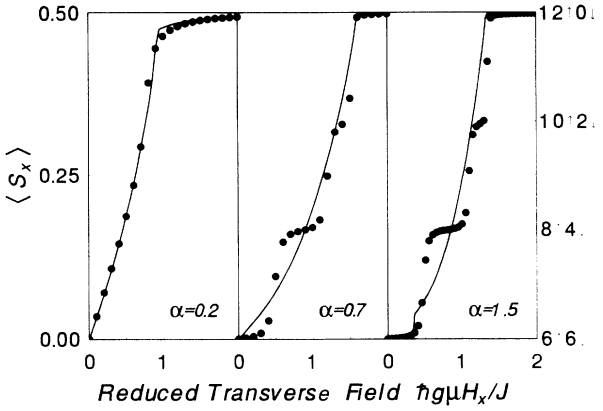

FIG. 11. Magnetization per site in units of $\hbar\mu$ for three values of the anisotropy parameter and for the transverse field. The continuous lines represent the results of our variational calculation and the black circles the computer simulation. The stepped appearance of the results of the latter are due to the finite size of the sample. The scale at the right represents the magnetization in units of spins up and down for the 12 spins of the sample.

VII. CONCLUSIONS

Our main objective in this paper is to introduce the method and to show that it constitutes a valuable tool in the study of the Heisenberg model with magnetic field in one or more dimensions. Most of the calculations and all the specific results presented here are valid for the linear chain. The general formalism, however, is not restricted to one dimension. On the contrary, there are sound arguments indicating that precision must increase dramatically with the lattice dimension.[23,28] Whereas the linear chain is the weaker case for our analytic variational approach, it is the only one that allows for a complete and reliable numerical solution for the ground state with finite magnetic field. Hence, the success of our trial function in one dimension constitutes the most stringent test for the general approach put forward in Secs. II and III.

A detailed study of the ground-state properties of the anisotropic Heisenberg antiferromagnet with higher dimensionalities is now in progress, and the results are planned to be published elsewhere. Our scope at this stage is simply to show the accuracy and reliability of the formalism. Beside its precision and mathematical simplicity, the method has the important advantage of accounting for the different magnetic phases and their transitions with a single trial function having a compact mathematical expression.

ACKNOWLEDGMENTS

This work has received financial support from FONDECYT and DTI.

[1]D. Vaknin, S. K. Sinha, D. E. Moncton, D. C. Johnston, J. M. Newsam, C. R. Safinya, and H. E. King, Jr., Phys. Rev. Lett. **58**, 2802 (1987).
[2]M. Sato, S. Shamoto, J. M. Tranquada, G. Shirane, and B. Kleiner, Phys. Rev. Lett. **61**, 1317 (1988).
[3]G. Shirane *et al.*, Phys. Rev. Lett. **59**, 1613 (1987).
[4]E. Manousakis, Rev. Mod. Phys. **63**, 1 (1991)
[5]D. Gottlieb and M. Lagos, Solid State Commun. **79**, 551 (1991).
[6]D. A. Huse and V. Elser, Phys. Rev. Lett. **60**, 2531 (1988).
[7]D. Huse, Phys. Rev. B **37**, 2380 (1988).
[8]H.Yokoyama and H. Shiba, J. Phys. Soc. Jpn. **56**, 1940 (1987).
[9]E. Manousakis, Phys. Rev. B **40**, 4904 (1988).
[10]A. Auerbach and D. P. Arovas, Phys. Rev. Lett. **61**, 617 (1988).
[11]D. C. Mattis and C. Y. Pan, Phys. Rev. Lett. **61**, 463 (1988).
[12]R. Wang, Phys. Rev. B **43**, 3786 (1991).
[13]T. Pang, Phys. Rev. B **43**, 3362 (1991).
[14]G. Gómez-Santos, Phys. Rev. B **41**, 6788 (1990).
[15]H. Bethe, Z. Phys. **71**, 205 (1931).
[16]R. Orbach, Phys. Rev. **112**, 309 (1958).
[17]J. des Cloiseaux and M. Gaudin, J. Math. Phys. **7**, 1384 (1966).
[18]H-Q Ding, J. Phys. Condens. Matter **2**, 7979 (1990).
[19]M. Lagos and G. G. Cabrera, Solid State Commun. **67**, 221 (1988).
[20]M. Lagos, M. Kiwi, E. R. Gagliano, and G. G. Cabrera, Solid State Commun. **67**, 225 (1988).
[21]M. Lagos and G. G. Cabrera, Phys. Rev. B **38**, 659 (1988).
[22]D. Gottlieb and M. Lagos, Phys. Rev. B **39**, 2960 (1989).
[23]G. G. Cabrera, M. Lagos, and M. Kiwi, Solid State Commun. **68**, 225 (1988).
[24]D. Gottlieb, M. Lagos, K. Hallberg, and C. Balseiro, Phys. Rev. B **43**, 13 668 (1991).
[25]M. Lagos, Solid State Commun. **77**, 597 (1991).
[26]D. Gottlieb and V. Díaz, Phys. Rev. **44**, 2803 (1991).
[27]M. Montenegro and D. Gottlieb, J. Phys. Condens. Matter **3**, 8641 (1991).
[28]D. Gottlieb, M. Lagos, and M. Montenegro, Solid State Commun. **81**, 729 (1992).
[29]T. Barnes, D. Kotchan, and E. S. Swanson, Phys. Rev. B **39**, 4357 (1989).
[30]E. Dagotto and A. Moreo, Phys. Rev. B **31**, 865 (1985).
[31]E. Gagliano, E. Dagotto, A. Moreo, and F. Alcaraz, Phys. Rev. B **34**, 1677 (1986).